Synthesis and Characterization of Polypyrrole/Graphite Oxide nanocomposites and Study of Electrical Properties

Kousik Dutta[*]

Assistant Professor in Physics

Department of Physics, Behala College, Parnashree; Kolkata- 700060; INDIA Author for

Reduction of the nanocomposite of the conductive polymer composite in the GO/conductive polymer imparts excellent mechanical, thermal, electrical and electrochemical properties to the composite. Therefore, the GO/conductive polymer has become the research direction of new functional materials. The polypyrrole/GO composite was prepared by in-situ polymerization using graphite oxide as the matrix and polypyrrole as the guest of the difference layer. A series of conducting polymer composites of polypyrrole/graphite oxide (PPY/GO) were prepared by the incorporation of pyrrole in various proportions. Polymer composites were characterized by XRD, SEM, four probe method, DC conductivity. PPy/GO composites showed crystalline nature with hexagonal structure. Direct current electrical conductivity values of all the samples have been measured. The temperature dependence dc conductivity of the nanocomposite follows Mott's three-dimensional variable range hopping. The alternating current (ac) conductivity suggests correlated barrier hopping of conduction process. The conductivity relaxation time varies in the range of 10^{-5}–10^{-7} Sec.

I. INTRODUCTION:

Conducting polymers and different fillers have been studied for many years for their independent electrical [1], optical [2,3] and mechanical [4] properties. Recently the semiconducting properties of conjugated polymers with carbon fillers [5] have brought new prospects and applications in modern technologies, such as chemical sensors [6,7], electrochromic displays [8], electronic devices [9], secondary batteries [10], etc. Among the different conjugated polymers, polypyrrole (PPY) has dragged the attention of researchers for the application in electronics and electric devices due to its good conductivity and stability. PPY shows its capability to store electrical charges. The stored electrical charges can be recovered upon demand, for that reason PPY can be considered as a good candidate of super-capacitors [11–15]. Han and Lu reported [16] the electrical conductivity of the graphite oxide/polypyrrole composites and the conductivity was found 7 S cm^{-1}. Yuan and his group reported the synthesis and characterization of SnO$_2$/PPy composite for lithium-ion battery where nanosize conducting PPy particles were uniformly coated onto the surface of the SnO$_2$ powder. The composite demonstrated significantly improved capacity and cycle durability compared with the bare SnO$_2$ electrode [17]. Recently, Park et al. [18] have built PPY/graphite electrodes with a rather high specific capacitance by chemical polymerization of pyrrole on the surface of a porous graphite fiber matrix, using an elegant, sequential dipping method. The prepared electrodes showed a specific capacitance of ﹍400 F g^{-1} and a Coulombic efficiency of 96–99%. Graphite is one of the widely studied carbon fillers due to its unique properties like good conductivity [18,19] better adsorption capability and low cost compared to other fillers. Literary survey reveals that there is dearth of reports on thermal

stability, DC conductivity and electrochemical studies especially in case of chemically synthesized PPY/GO composites. Therefore, in the present study we have reported the synthesis, characterization, DC conductivity of PPy/GO composites in details.

The significant improvement in electrical conductivity arising from the increase of filler content is observed for most of composites and it is explained by the percolation transition of the conductive network formation. The percolation values for a critical transition varies system to system. In most of the cases relatively large quantities of filler were needed to reach the critical percolation values. Polypyrrole (PPY) is one of the most studied conducting polymer because of its good electrical conductivity, environmental stability and relative easy synthesis [20]. In the past decade, the intercalation of polypyrrole into layered materials has received a great deal of attention because the confinement of polypyrrole molecules was expected to result in high degree of ordering and enhanced charge carrier mobility. Blending polymer with conducting fillers such as natural graphite flake, carbon black, and metal powders, to prepare electrically conducting composites has been extensively investigated in the past few decades.

Graphite is well known to be a layered material with ac axis lattice constant of 0.66nm. [21] Carbon atoms within a layer are covalently bonded by much weaker van der Waals force. Three types of staking are known to exists in graphite. ABAB, ABCABC, and AAAA types. The most common form of graphite has the ABAB staking ,and natural graphite also contains the ABCABC staking in a small ratio. In the natural graphite, the c-c bond length is 1.42 ° A within the sheets are separated by 3.35 ° A. The inter layer spacing is approximately the sum of the Van der waals radii of the carbon atom. The AAAA staking has not been observed so far in the natural graphite. It is expected both physiochemical properties and electrical conductivity can be improved in case that PPY is intercalated into the interlayer space of graphite. Nevertheless it is difficult for the organic or polymer to enter the interlayer gallery of graphite due to the very small gallery spacings between the graphite interlayers. In this connection some modification of the graphite has to be performed to prepare polymer/graphite oxide nanocomposite. [22,23] It is understood that natural graphite flake could be intercalated by various chemical methods to form the graphite intercalation compounds(GICs). Co intercalation of the monomer into the GICs then can be achieved and subsequent polymerization could lead to intercalated polymer/graphite oxide composites. Natural graphite flakes provide good electrical conductivity and layered structure with a c axis lattice constant, which indicates interplanar spacing, of 0.66 nm. Since there are no reactive ion groups on the graphite layers, it is difficult to prepare the polymer graphite nanocomposites via ion exchange reaction in order to intercalate the monomer

into the graphite sub layers. On the other hand graphite oxide is a pseudo two dimensional solid in bulk form, possesses hydroxyl, carbonyl and other functional groups. these groups makes graphite oxide easily absorb polar molecule and polar polymers by different meance to form graphite oxide intercalated nanocomposites. The graphite oxide maintains layered structure similar to natural flake graphite but with larger layer spacing.

monomers and macromolecules are able to intercalate into the galleries of graphite oxide. It is expected both physiochemical properties and electrical conductivity can be improved in case that PPY is intercalated into the interlayer space of graphite oxide. In the present work, characterization and electrical properties of polypyrrole-graphite oxide are presented in details.

II. EXPERIMENTAL:

A. **Chemical and Reagents:** The graphite used in this study is natural flake graphite supplied from Alfa Aesar Company. pyrrole and ammonium peroxydisulphate (APS)($(NH_4)S_2O_8$) are purchased from E. Merck (India). Pyrrole(AR) is purified and stored at -15^0 C in a refrigerator

prior to use. APS oxidant, concentration sulfuric acid, hydrogen peroxide, hydrochloric acid is used as received.

Graphite oxide sample is prepared by Hammers method [24] with some modification. Graphite powder is put into a 500 ml flask containing a quantity of fuming nitric acid and 98 % H_2SO_4 and stirred for an one hour under ice bath, then a quantity of $KMmO_4$ is added into the solution After half an hour the solution temperature is gradually raised to 40 degree centigrade and maintained half an hour, then the product is reduced using H_2O_2 and wash several times using distilled water.
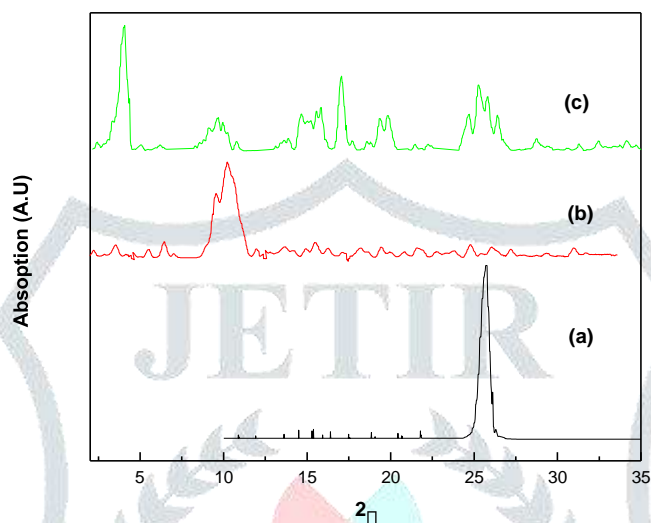

Fig 1. X-ray diffraction pattern of graphite (a), graphite oxide (b) PPY-graphite oxide nanocomposite (c) for sample S6

Table I. Amount of pyrrole (x ml), room temperature conductivity σ(RT), σ_0, T_0, density of states $N(E_F)$, hopping length R_{hop}, activation energy W_{hop}.

sample	X ml	σ (RT)(10^{-4}) (s/cm)	σ_0 (10^3) (s/cm)	T_0(10^7) (K)	$N(E_F)$(10^{20}) eV$_{-1}$cm$_{-3}$	R_{hop} A^0	W_{hop} (meV)
S1	0.3	5.02	16.50	11.50	1.50	24.7	170
S2	0.5	25.40	14.34	5.50	3.54	21.5	135
S3	0.7	325.84	5.01	0.125	150	9.01	64
S4	1	420.32	4.50	0.106	215	8.50	51
S5	3	561.45	3.85	0.065	278	7.63	40
S6	5	3250.52	3.05	0.0054	2019	6.02	22

B. Preparation of Polymer Nanocomposites:

For the preparation of the PPY- graphite oxide nanocomposite 50 mg of graphite oxide powder is taken at each time and selected volume of pyrrole is then added to the solution under sonication to get the pyrrole intercalated graphite oxide. After 6 hours APS solution maintaining pyrrole : graphite oxide mole ratio of 1:1.25 is added drop wise under sonication . The solution turned black after various time period.
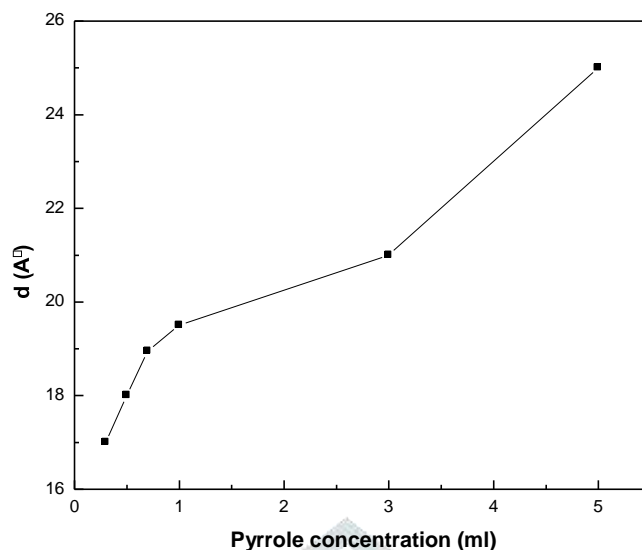
Fig. 2. The plot of interlayer spacing (d) versus pyrrole concentration

After 20 hours the resulting dispersion are centrifuged at 10000 r.p.m for 2 hour using REMI centrifuge instruments. The resulting nanocomposites are washed thoroughly with distilled water several times. The analogous PPY bulk powder is prepared using the same protocol describe above. Both nanocomposite and bulk powder were oven dried at 70^0 C for 48 hour. Compositions of different nanocomposite samples prepared are shown in Table I.

C. Characterization of the Polypyrrole-Graphite Oxide Nanocomposite

The X-ray powder diffraction studied are carried out with Philips Diffractometer in the range 0 to 35 using CuK radiation..The microstructure is obtained using scanning electron microscope (SEM). The temperature dependent dc conductivity is measured by the standard four-probe method using Keithley 2000 multimeter. The capacitance (C) and loss factor (D) as a function of frequency are measured by Agilent 4192A impedance analyzer up to the frequency range 10 MHz at different temperatures. The real part of the ac conductivity σ (ω) is determined by the relation σ (ω) = ω*DCt/A*, where *t* is the thickness and *A* is the area of the sample. All nanocomposite samples are pelletized by applying 6 ton pressure. The thickness of all nanocomposites sample (pellet) varies from 0.08–0.12 cm and the area of all sample are same (0.7854 cm^2).
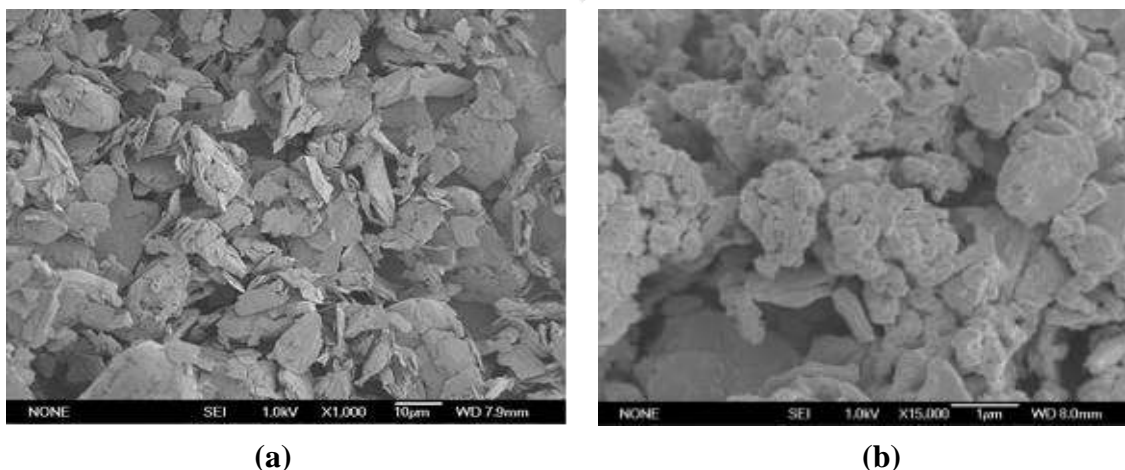

(a)   (b)

Fig. 3. Scanning electron micrograph of graphite oxide (a) and PPY-graphite oxide nanocomposite sample S6 (b).

III. RESULTS AND DISCUSSION:

The X-ray diffraction patterns of graphite, graphite oxide, and the graphite oxide-polypyrrole nanocomposites are shown in the Figure 1. The most intense peak of graphite at around $2\Theta = 25.6^0$ is observed corresponding to (001) plane. The diffractogram of graphite-oxide is appeared at $2\Theta = 10.3^0$. For graphite oxide-polyaniline samples the first peak shifts to the lower angle. The interlayer distance of these samples are estimated from Bragg's law, $2d \sin \Theta = \lambda$. The first peak (001) of graphite is shifted to lower angle in case of graphite oxide. The interlayer spacing of graphite is 3.46 Å, and for graphite oxide it is 8.75 Å which indicates the lattice expansion of graphite nanosheets. With increase of pyrrole concentration the interlayer spacing of graphite oxide increases as shown in the Figure 2. The increase of interlayer spacing with increasing pyrrole concentration clearly demonstrates the incorporation of pyrrole into the interlamellar spacing of graphite oxide. The maximum lattice expansion for the highest loading of pyrrole is 25.1 Å. The scanning electron micrographs of graphite oxide and nanocomposites (S6) are shown in the Figure 3. The micrograph of graphite oxide shows the sheet like morphology. The nanocomposites show the plate (sheet) like structure similar to the graphite oxide. The sizes of plates are very small compared to graphite oxide.

Room temperature conductivity (RT) for various compositions are shown in Table I. The graphite has electrical conductivity of about 10^4 S/cm due to the overlap of valence and conduction bands. Graphite oxide, although the layered structure of graphite is remained, the aromatic character of the planer graphite is lost and the electrical conductivity reduces. As a result of it, the conductivity of dry graphite oxide has one of only 10^{-6} S/cm. Therefore; the electrical conductivity of PPY/graphite oxide nanocomposites is expected to be very low. The dc conductivity increases with the increasing content of PPY. The relatively higher electrical conductivity arises mainly from doped PPY matrix. The enhancement of $\sigma(RT)$ is about four orders of magnitude for the highest fraction of PPY.
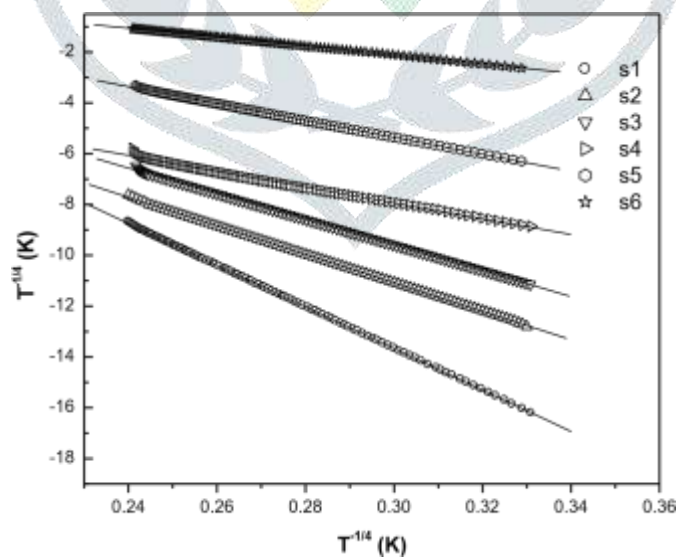

Fig. 4. Temperature variation of dc conductivity of the nanocomposites sample,respectively.The solid lines are fits to Eq.(1)

The temperature dependence of dc conductivity for nanocomposite samples are shown in Figure 4. The temperature dependence of conductivity $\sigma(T)$ of nanocomposites has been analyzed by the Mott's variable range hopping (VRH) model, [25]

$$\sigma(T) = \sigma_0 \exp(-(T_0/T)^\gamma) \qquad (1)$$

where σ_0 is the high temperature limit of conductivity and T_0 is Mott's characteristic temperature associated with the degree of localization of the electronic wave function. The exponent $\gamma = 1/(1+d)$ determines the dimensionality of the conducting medium.

The possible values of γ are 1/4, 1/3, and 1/2 for three, two, and one-dimensional systems, respectively. The plot of $\ln \sigma(T)$ against $T^{-1/4}$ indicates that three-dimensional (3D) charge transport occurs in the PPY-graphite oxide nanocomposites. The values of Mott's characteristic temperature T_0 and the pre exponential factor σ_0 are obtained from the slopes and intercepts of the Figure 4 and are given in Table I. The values of T_0 are very sensitive and decrease with increasing PPY content.

The characteristic temperature T_0 for three-dimensional hopping transport is given by

$$T_0 = 16/(kL^3 N(E_F)) \qquad (2)$$

where L is the localization length and $N(E_F)$ is the density of states at the Fermi level. As T_0 is inversely proportional to L, the degree of disorder of the systems reduces with lowering of T_0. The value of T_0 decreases as sample conductivity increases. The density of states, $N(E_F)$ are calculated by considering the charge transport primarily arising from conducting PPY phase and assuming localization length of the polypyrrole monomer unit about 3 Å.
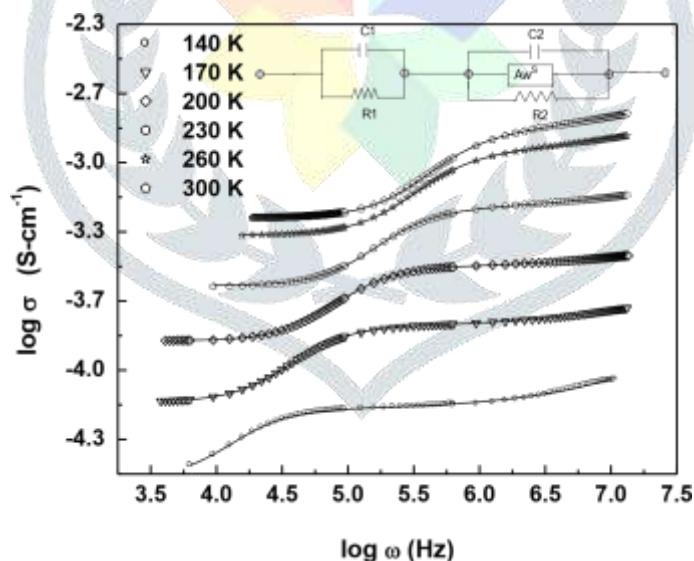

Fig. 5. Frequency dependence to total conductivity at different temperatures of samples S2.

The higher value of density of states at the Fermi level is also consistent with the increase of dc conductivity with increase of PPY content.

The average hopping distance R_{hop} between two sites and the activation energy W_{hop} are

$$R_{hop} = (3/8)(T_0/T)^{1/4}L \qquad (3)$$
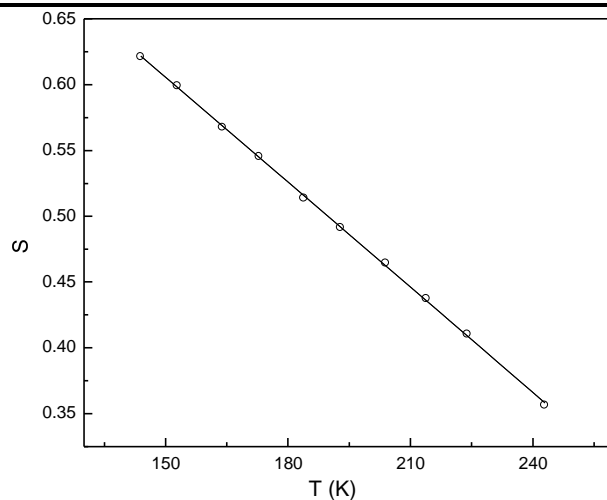
$$W_{hop} = (1/4)kT(T_0/T)^{1/4} \qquad (4)$$

Fig. 6. Frequency exponent (S) versus temperature (T) of sample S2. The solid curve are fits to Eq.(6)

At room temperature the average hopping distance for sample S1 is about 24 Å and it reduces to about 6 Å for the highest content of PPY. This corresponds to about 8–2 monomer units in length. The estimated activation energies for hopping as shown in Table I are in the range of 170–22 meV.
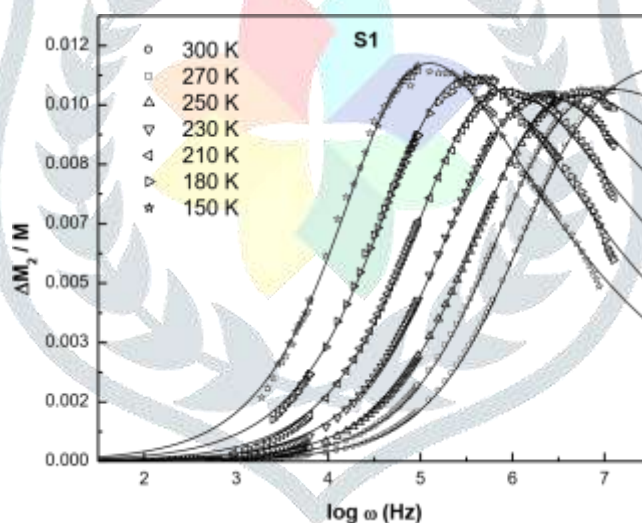

Fig. 7. Imaginary part of modulus of nanocomposite S2 at different temperatures.

Both the hopping distance and activation energy decreases as conductivity increases. The closer approaches of hopping sites enhances the conductivity. The increase of PPY content expands interlamellar space which is comparable to the average hopping distant. This confirms PPY in the nanocomposites plays an important factor in the dc conduction process.

The conductivity as a function of frequency, $\sigma(\omega)$ provides the detailed knowledge about the transport mechanism of charge carriers. The most prominent effect of $\sigma(\omega)$ is only observed for the sample S2 within the available frequency and temperature intervals. Figure 5 shows the frequency dependence of conductivity of sample S2 at various temperatures. The conductivity increases after certain frequency. This is true for disordered systems in which hopping mechanism dominates. The moving of smaller and smaller distance of charge carriers with increase of

frequency leads to enhancement of conductivity. The ac conductivity is generally described by the following power law

$$\sigma(\omega) = \sigma_{dc} + A\omega^s \qquad (5)$$

where σ_{dc} is the dc conductivity and A is a constant depending on temperature. The frequency exponent S lies between 0 and 1. Such universal dynamic response is found in a variety of disordered materials. The values of S are estimated from the best-fitted data from the plots of log ($\sigma(\omega)$ - σ_{dc}). The calculated values of S are in the range of 0.35 to 0.63 for all the temperatures.
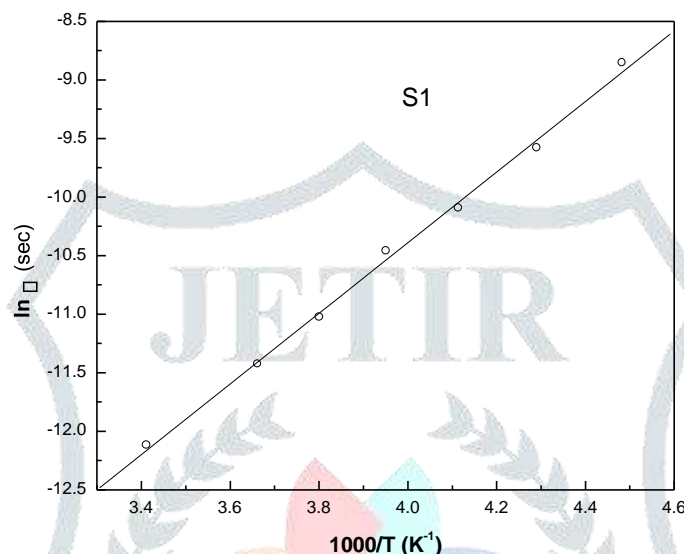

Fig. 8. Temperature variation of relaxation time (τ) of sample S2

     The microscopic conduction mechanisms of disordered systems are governed by two physical processes such as classical hopping and quantum mechanical tunneling of charge carriers over the potential barrier separating two energetically favorable centers in a random distribution. The exact nature of charge transport is mainly obtained experimentally from the temperature variation of exponent S. Temperature dependence of S for S2 is shown in Figure 6.The value of frequency exponent S decreases with increase of temperature. This behavior is only observed in correlated barrier hopping model. [26] The temperature dependence of S based on this model is

$$S = 1 - \frac{6kT}{W_M - kT \ln\left(\frac{1}{\omega\tau_0}\right)} \qquad (6)$$

where W_M is the effective barrier height at infinite intersite separation, τ_0 is the characteristic relaxation time, and k is the Boltzmann constant. The values of W_M and τ_0 are obtained by the best fitted parameters to Eq.(6) at a frequency of 100 kHz. Figure 6 exhibits that the experimental values of S are in good agreement with theoretical model. The estimated barrier height is 310 meV and relaxation time is 6.4×10^{-7} sec. The electric modulus is very useful to suppress the extrinsic effect such as electrode polarization. The characteristic features of conductivity relaxation are obtained from the electric modulus *(M)* .The complex electric modulus *M** is defined as[27,28]

$$M^*(\omega) = M_1 + iM_2 = \frac{1}{\varepsilon^*(\omega)} = \frac{\varepsilon_1 + i\varepsilon_2}{\varepsilon_1^2 + \varepsilon_2^2} \qquad (7)$$

Figure 7 shows the frequency spectrum of the imaginary part (M_2) of electric modulus of sample S2 at different temperatures. The broad peaks are observed and are skewed at higher frequency. The frequency at which the maximum of M_2 occurs gives the conductivity relaxation. The loss peak moves to higher frequency as temperature increases. The relatively larger width and asymmetrical nature of M_2 peak has been described by the more generalized Hevriak-Negami (HN) function,[29]

$$M^{\bullet}(\omega) = M_{\infty}\left[1 - \frac{1}{(1+(i\omega\tau)^{\alpha})^{\beta}}\right]$$

Where τ is the conductivity relaxation time which is given at the frequency of maximum loss peak. M_{∞} is electric modulus at higher frequency. The parameter β describes the distribution of the relaxation time of the system. Debye relaxation is obtained for $\alpha = \beta = 1$. The best-fitted curves are obtained for $.\alpha = 058\text{--}0.68$ and $\beta = 0.10\text{--}0.31$ in the entire temperature interval of 220 K–270 K. The relaxation time as a function of temperature is shown in Figure 8

The variation of relaxation time with temperature can be described by Arrhenius plot and is given by

$$\tau = \tau_0 \exp(E/kT)$$

where τ_0 is the pre-exponential factor, E is the activation energy for the relaxation process. The linear behavior of ln versus $1/T$ confirms Arrhenius type relaxation process. The slope of the straight line in Figure 8 yields the activation energy of 305 meV, which is almost similar to the value of barrier height.

IV. CONCLUSION

The incorporation of conducting polypyrrole modifies electronic structure of the host graphite oxide. Electrical conductivity is dramatically modified compared to graphite oxide. The variation of dc conductivity with temperature satisfies three dimensional variable range hopping conduction process. Ac conductivity reveals correlated barrier hopping for lower content of polypyrrole.

IV. REFERRENCE:

[1] P.V. Notingher, D. Panaitescu, Z. Vuluga, M. Iorga, H. Paven, D. Florea, J. Opt. Adv. Mater. 8 (2006) 687.
[2] J. Maiti, S.K. Dolui, J. Lumin. 129 (2009) 611.
[3] P. Somani, S. Radhakrishnan, Mater. Chem. Phys. 76 (2002) 15.
[4] I.K. Moon, C.S. Choi, N. Kim, J. Polym. Sci., Part B: Polym. Phys. 47 (2009) 1695.
[5] G.J. Lu, D. Wu, Mater. Chem. Phys. 104 (2007) 240.
[6] F. Cakara, M.R. Moroglua, H. Cankurtaran, F. Karaman, Sens. Actuators B 145 (2010) 126.
[7] J. Maiti, B. Pokhrel, R. Boruah, S.K. Dolui, Sens. Actuators B 141 (2009) 447.
[8] P. Somani, A.B. Mandale, S. Radhakrishnan, Acta Mater. 48 (2000) 2859.
[9] K. Mylvaganam, L.C. Zhang, Recent Pat. Nanotechnol. 1 (2007) 59.

[10] K. Ghanbari, M.F. Mousavi, M. Shamsipur, H. Karami, J. Power Sources 170 (2007) 513.

[11] G. Dione, M.M. Dieng, J.J. Aaron, H. Cachet, C. Cachet, J. Power Sources 170 (2007) 441.

[12] F.R. Kalhammer, Solid State Ionics 135 (2000) 380.

[13] K.S. Ryu, Y. Lee, K.S. Han, M.G. Kim, Mater. Chem. Phys. 84 (2004) 380.

[14] J. Zang, S.J. Bao, C.M. Li, H. Bian, X. Cui, Q. Bao, C.Q. Sun, J. Guo, K. Lian, J. Phys.Chem. C 112 (2008) 14843.

[15] K. Jurewicz, S. Delpeux, V. Bertagna, F. Béguin, E. Frackowiak, Chem. Phys. Lett. 347 (2001) 36.

[16] Y. Han, Y. Lu, Carbon 45 (2007) 2394.

[17] L. Yuan, J. Wang, S.Y. Chew, J. Chen, Z.P. Guo, L. Zhao, K. Konstantinov, H.K. Liu, J. Power Sources 174 (2007) 1183.

[18] J.H. Park, J.M. Ko, O. Park, D.W. Kim, J. Power Sources 105 (2002) 20.

[19] S. Konwer, B. Pokhrel, S.K. Dolui, J. Appl. Polym. Sci. 116 (2009) 1138.

[20] T. Skothemin, R. Elsenbaumer, Handbook of Conducting Polymers, Marcel Dekker, New York, 1998.

[21] Cao NZ, Shen WC, Wen SZ, Liu YJ, Wang ZD, Inagaki M. The factors influencing the porous structure of expanded graphite. Mater Sci Eng (Chinese)**14**, 226 (1996)

[22] Shioyama H, Tatsumi K, Iwashita N. Synth Met **96**, 229-33 (1998).

[23] Xiao M, Sun L, Liu J, Li Y, Gong Kc. Polymer **43(8)**, 2245-8 (2002).

[24] William S.Hummers, Jr.and Richard E.Offeman, *J. Am. Chem. Soc.* 80, 1339 **(1958)**. **[25]** N.F.Mott and E.Davis (ed.), Electronic Process in Non Crystalline Materials, 2nd edn.,Oxford, Clarendon **(1979)**.

[26] S.R.Elliott, *Adv. Phys.* 37, 135 **(1987)**.

[27] P.B.Macedo, C.T.Moynihan, and R.A.Bose, *Phys. Chem. Glasses* 13, 171 **(1972)**.

[28] F.S.Howell, R.A.Bose, P.B.Macedo, and C.T.Moynihan, *J. Phys.Chem.* 78, 639 **(1974)**.

[29] S.Havriliak and S.Negami, *Polymer* 8, 161 **(1967)**